

Supplementary information

Two fluorescent lead phosphonates for highly selective sensing of nitro aromatics (NACs), Fe^{3+} and MnO_4^- ions

Bo Xing, Huan-Yu Li, Yan-Yu Zhu, Zhou Zhao, Zhen-Gang Sun*, Dan Yang and Jing Li

School of Chemistry and Chemical Engineering, Liaoning Normal University, Dalian 116029, P. R. China

Table S1. Selected Bond Distances (\AA) and Angles (deg) for **1**

Pb(1)–O(2)#1	2.290(4)	P(1)–O(3)	1.602(4)
Pb(1)–O(5)#2	2.348(4)	P(1)–C(3)	1.812(6)
Pb(1)–O(4)	2.446(4)	P(2)–O(4)	1.489(4)
Pb(1)–O(1)#3	2.578(4)	P(2)–O(5)	1.493(4)
P(1)–O(1)	1.500(4)	P(2)–O(6)	1.601(4)
P(1)–O(2)	1.507(4)	P(2)–C(16)	1.806(5)
O(2)#1–Pb(1)–O(5)#2	97.16(14)	O(4)–P(2)–O(5)	117.5(2)
O(2)#1–Pb(1)–O(4)	84.17(14)	O(4)–P(2)–O(6)	112.6(2)
O(5)#2–Pb(1)–O(4)	81.92(13)	O(5)–P(2)–O(6)	103.9(2)
O(2)#1–Pb(1)–O(1)#3	86.08(13)	O(4)–P(2)–C(16)	108.6(3)
O(5)#2–Pb(1)–O(1)#3	79.83(13)	O(5)–P(2)–C(16)	110.1(3)
O(4)–Pb(1)–O(1)#3	158.04(13)	O(6)–P(2)–C(16)	103.2(2)
O(1)–P(1)–O(2)	117.7(2)	C(2)–O(3)–P(1)	122.6(6)
O(1)–P(1)–O(3)	106.0(2)	P(2)–O(4)–Pb(1)	146.1(2)
O(2)–P(1)–O(3)	108.8(2)	C(17)–O(6)–P(2)	120.5(5)
O(1)–P(1)–C(3)	109.2(2)	P(1)–O(2)–Pb(1)#4	128.5(2)
O(2)–P(1)–C(3)	108.7(3)	P(1)–O(1)–Pb(1)#5	136.2(2)
O(3)–P(1)–C(3)	105.8(3)	P(2)–O(5)–Pb(1)#6	139.6(2)
Symmetry transformations used to generate equivalent atoms: #1 x – 1, y + 1, z, #2 x – 1, y , z, #3 x – 2, y + 1, z, #4 x + 1, y – 1, z, #5 x + 2, y – 1, z, #6 x + 1, y, z.			

Table S2. Selected Bond Distances (\AA) and Angles (deg) for 2

Pb(1)–O(4)#1	2.403(8)	Pb(3)–O(6) #4	2.517(5)
Pb(1)–O(11)	2.406(6)	Pb(3)–O(18)	2.731(6)
Pb(1)–O(1)	2.513(5)	P(1)–O(2)	1.478(6)
Pb(1)–O(17)#2	2.727(6)	P(1)–O(1)	1.515(6)
Pb(1)–O(10)	2.740(6)	P(1)–O(3)	1.603(7)
Pb(2)–O(2)	2.266(6)	P(2)–O(5)	1.484(8)
Pb(2)–O(16) #3	2.368(6)	P(2)–O(6)	1.499(5)
Pb(2)–O(16) #5	2.368(6)	P(2)–O(4)	1.572(8)
Pb(2)–O(7)	2.378(5)	P(3)–O(8)	1.495(6)
Pb(3)–O(8)	2.309(6)	P(3)–O(7)	1.518(5)
Pb(3)–O(19)	2.386(5)	P(3)–O(9)	1.594(6)
O(4)#1–Pb(1)–O(11)	84.9(3)	O(19)–Pb(3)–O(18)	50.89(17)
O(4)#1–Pb(1)–O(1)	110.2(2)	O(6)#4–Pb(3)–O(18)	123.19(17)
O(4)#1–Pb(1)–O(17)#2	146.0(2)	O(2)–P(1)–O(3)	111.4(4)
O(11)–Pb(1)–O(17)#2	78.6(2)	O(1)–P(1)–O(3)	105.6(4)
O(1)–Pb(1)–O(17)#2	95.11(19)	O(5)–P(2)–O(6)	114.6(4)
O(4)#1–Pb(1)–O(10)	69.7(2)	O(5)–P(2)–O(4)	97.3(5)
O(11)–Pb(1)–O(10)	49.60(18)	O(6)–P(2)–O(4)	110.6(4)
O(2)–Pb(2)–O(16)#3	79.2(2)	O(8)–P(3)–O(7)	114.7(3)
O(2)–Pb(2)–O(7)	80.3(2)	O(8)–P(3)–O(9)	113.1(4)
O(16)#3–Pb(2)–O(7)	86.6(2)	O(7)–P(3)–O(9)	105.4(4)
O(2)–Pb(2)–O(14)	90.1(3)	P(1)–O(1)–Pb(1)	134.3(3)
O(16)#3–Pb(2)–O(14)	158.7(2)	P(1)–O(2)–Pb(2)	146.2(4)
O(7)–Pb(2)–O(14)	73.31(19)	P(2)–O(4)–Pb(1)#1	121.2(5)
O(8)–Pb(3)–O(19)	89.7(2)	P(2)–O(6)–Pb(3)#4	136.1(3)
O(8)–Pb(3)–O(6)#4	79.26(19)	C(43)–O(16)–Pb(2)#5	108.2(5)
O(19)–Pb(3)–O(6)#4	78.61(18)	C(43)–O(17)–Pb(1)#2	110.9(5)

Symmetry transformations used to generate equivalent atoms: #1 – x + 1, – y + 2, – z,
#2 – x + 2, – y + 1, – z, #3 x – 1, y, z, #4 – x + 1, – y + 2, – z + 1, #5 x + 1, y, z.

Table S3. The ICP result of filtrate.

Compounds	Units	Elements	
		Fe	Mn
1	ppm	1.4826	0.8516
2	ppm	1.9319	0.0413

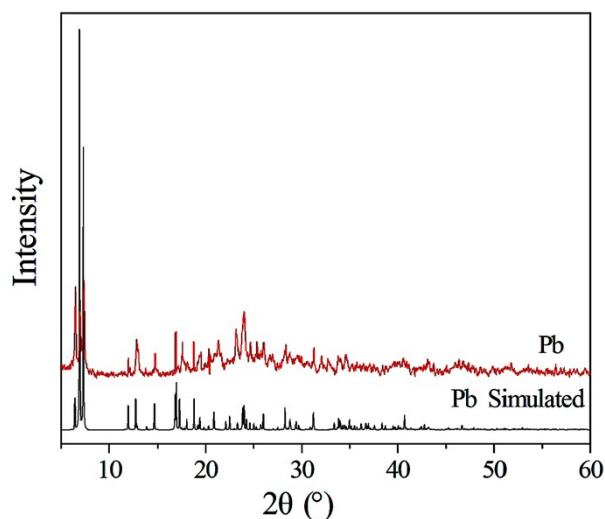


Fig. S1 The experimental powder XRD pattern and the simulated XRD pattern of compound **1**.

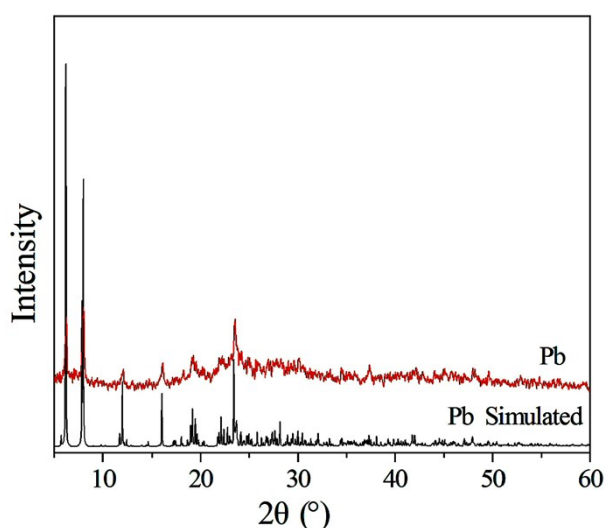


Fig. S2 The experimental powder XRD pattern and the simulated XRD pattern of compound **2**.

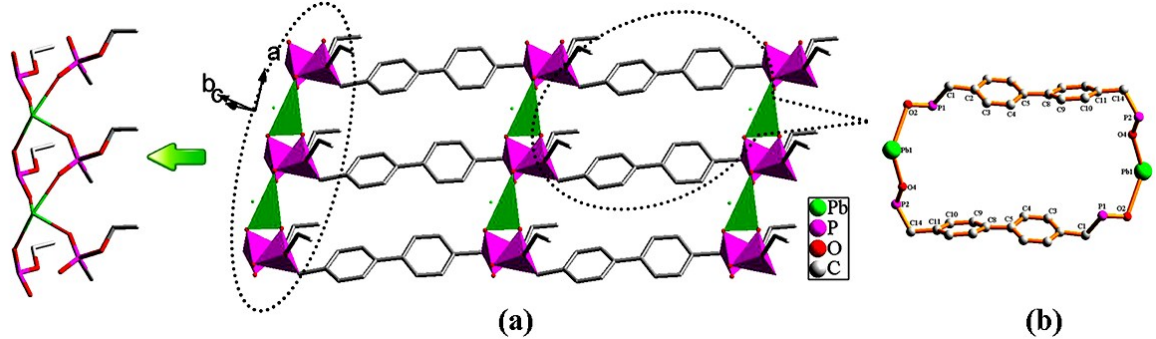


Fig. S3 (a) A 2D layer structure of compound **1** viewed in *ab*-plane; (b) the 30-atom windows in compound **1**.

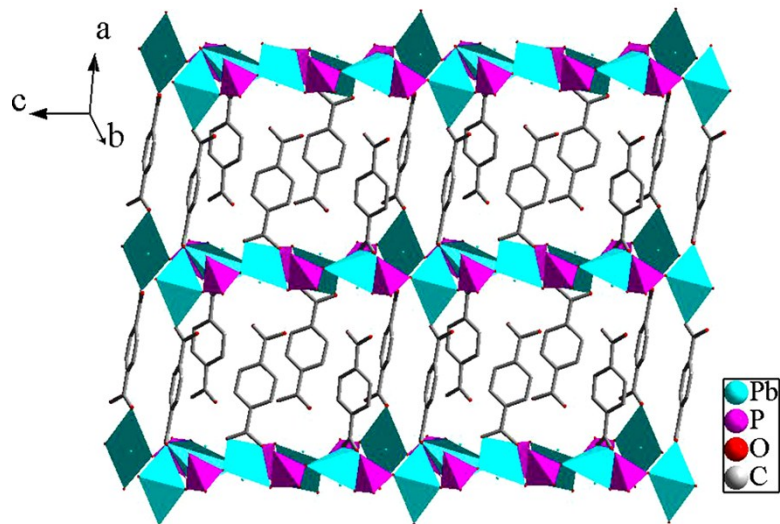


Fig. S4 The double layer structure of compound **2** viewed in *ac*-plane.

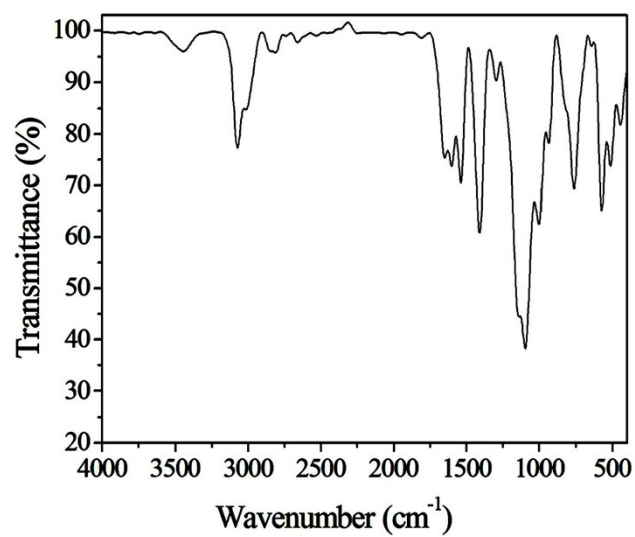


Fig. S5 The IR spectrum of compound **1**.

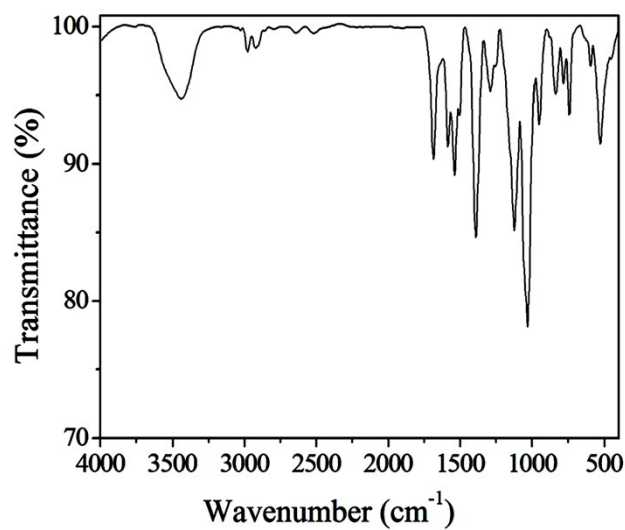


Fig. S6 The IR spectrum of compound **2**.

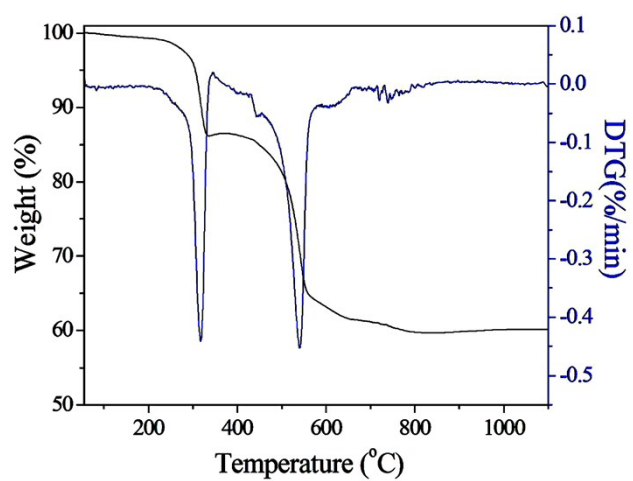


Fig. S7 The TG–DTG curves (10 K/min) of compound **1**.

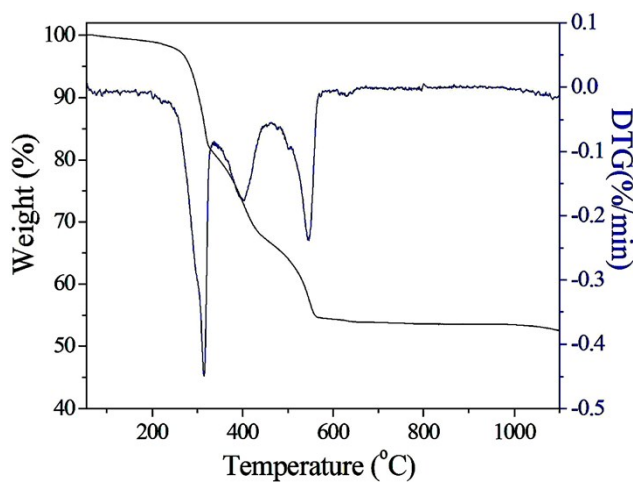


Fig. S8 The TG–DTG curves (10 K/min) of compound **2**.

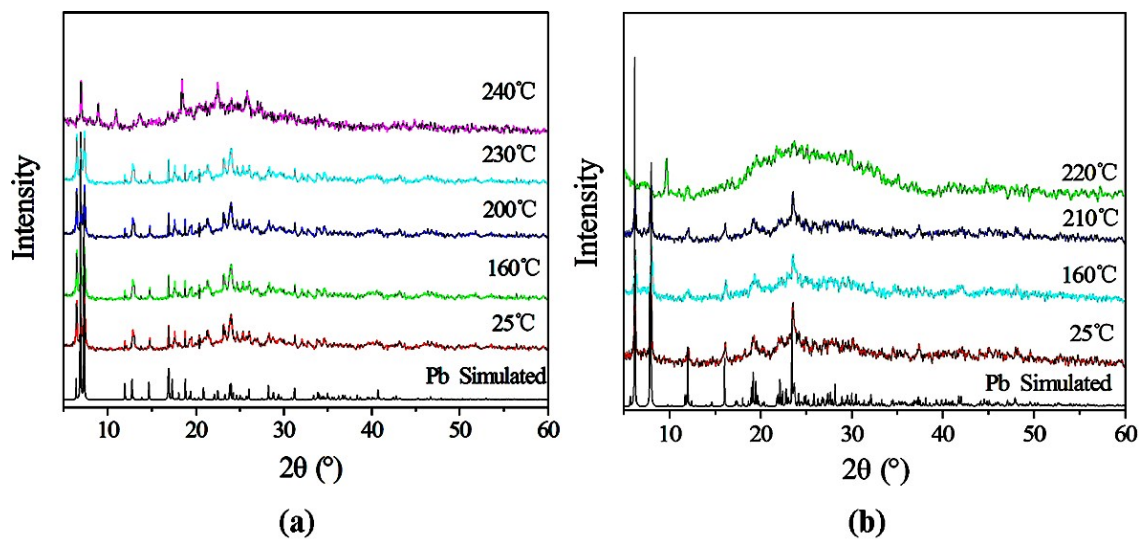


Fig. S9 The PXRD patterns for (a) **1** on heating from 25 to 240 °C and (b) **2** on heating from 25 to 220 °C.

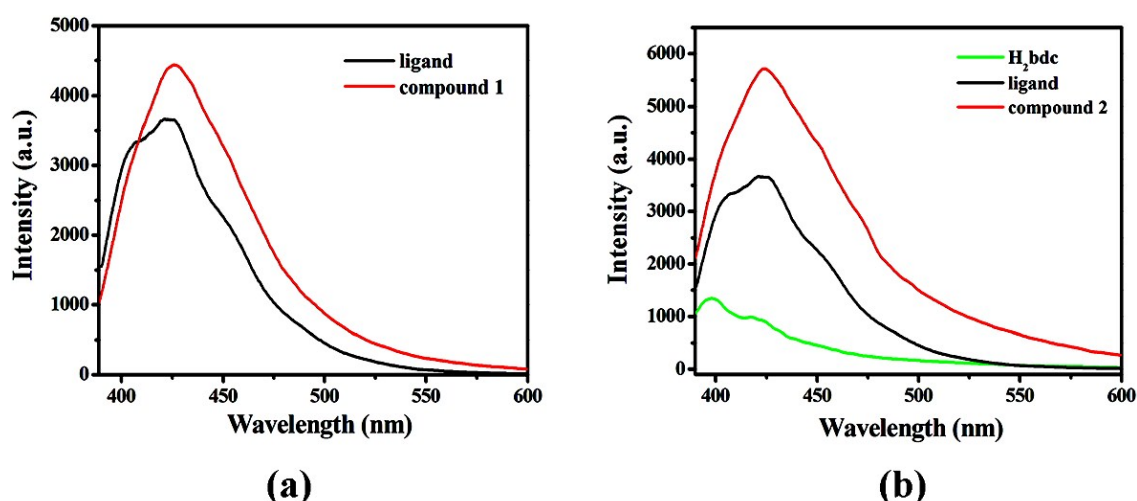


Fig. S10 The solid-state emission spectra of compound **1** (a) and compound **2** (b) at room temperature.

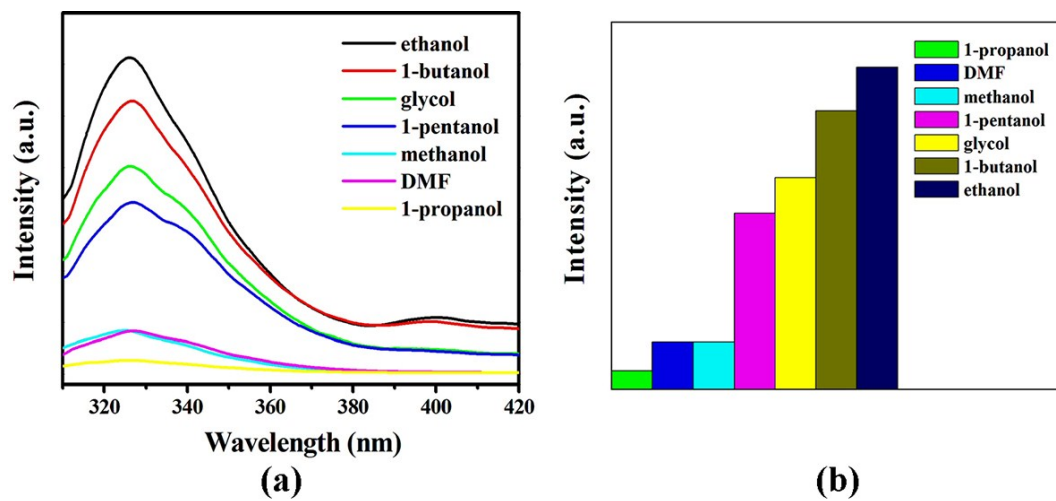


Fig. S11 The emission spectra of (a, b) compound **1** in various solvents at room temperature.

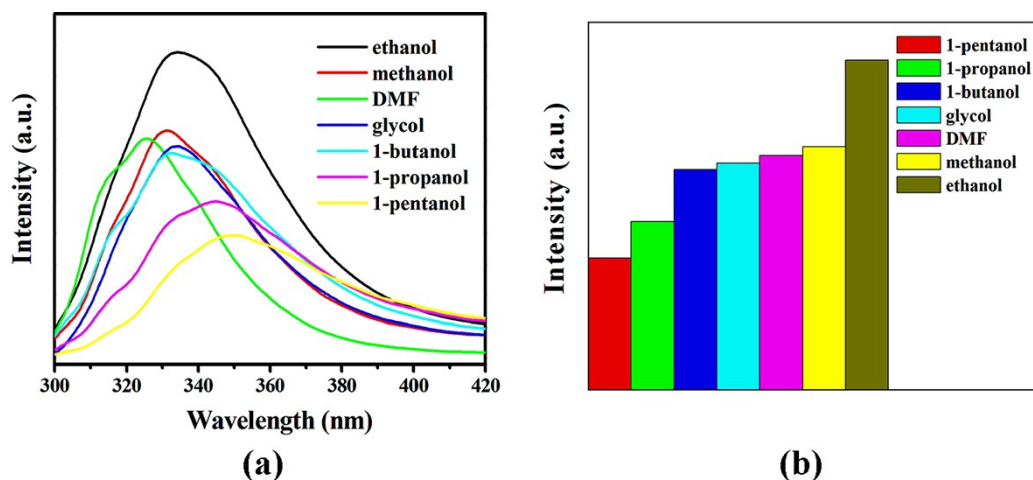


Fig. S12 The emission spectra of (a, b) compound **2** in various solvents at room temperature.

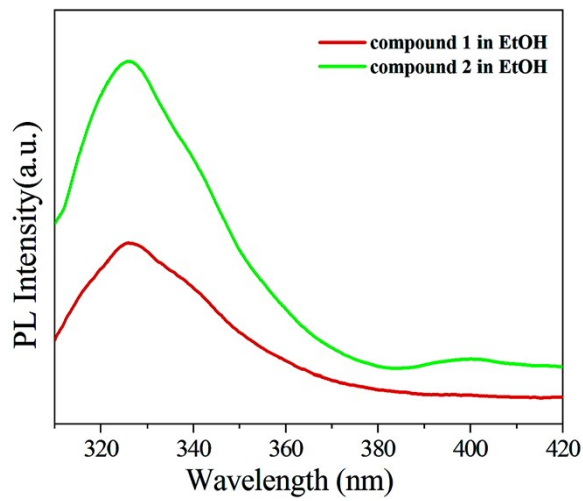


Fig. S13 The room temperature emission spectra of compounds **1** and **2** in ethanol.

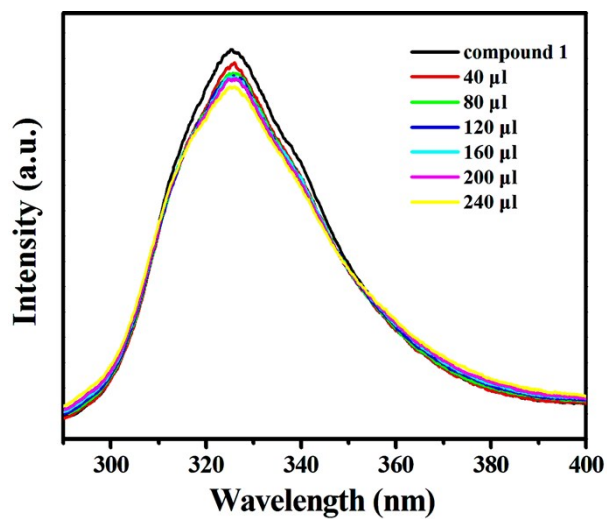


Fig. S14 The fluorescence properties of compound **1** suspension in the presence of various contents of nitromethane.

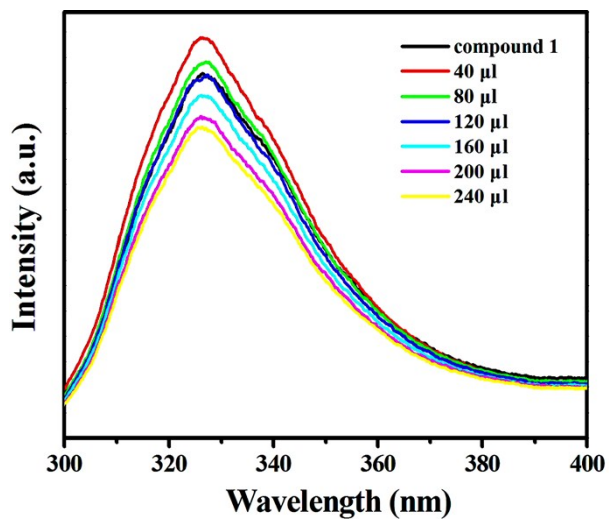


Fig. S15 The fluorescence properties of compound 1 suspension in the presence of various contents of m-dinitrobenzen.

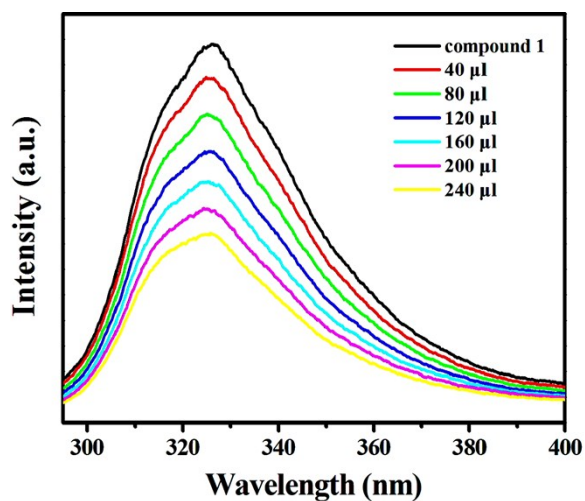


Fig. S16 The fluorescence properties of compound 1 suspension in the presence of various contents of o-nitrophenol.

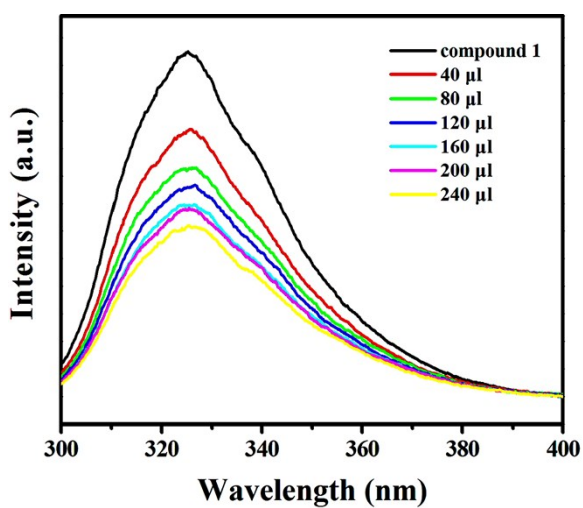


Fig. S17 The fluorescence properties of compound **1** suspension in the presence of various contents of 2,6-dinitrotoluene.

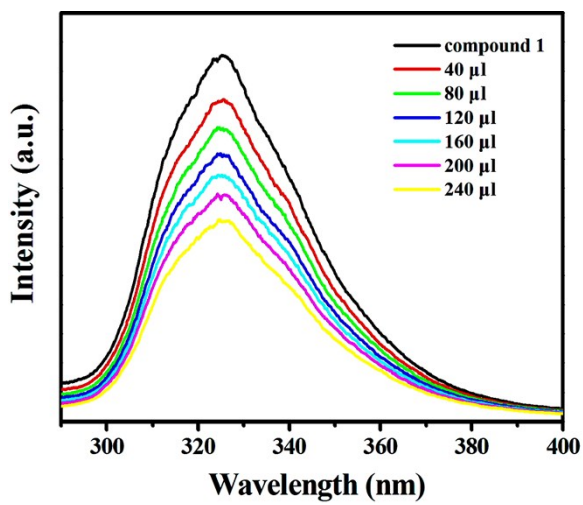


Fig. S18 The fluorescence properties of compound **1** suspension in the presence of various contents of nitrobenzene.

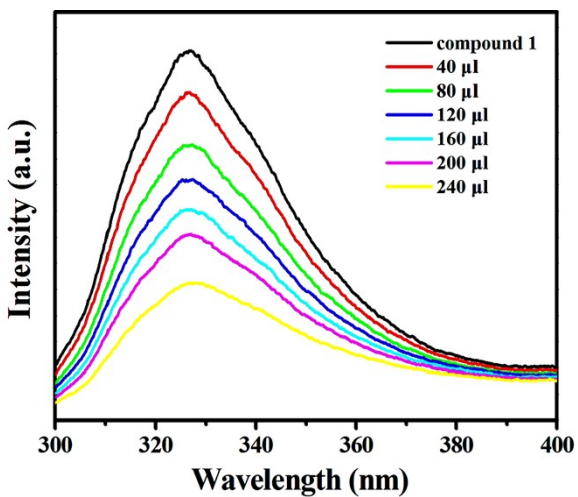


Fig. S19 The fluorescence properties of compound 1 suspension in the presence of various contents of 4-nitrotoluene.

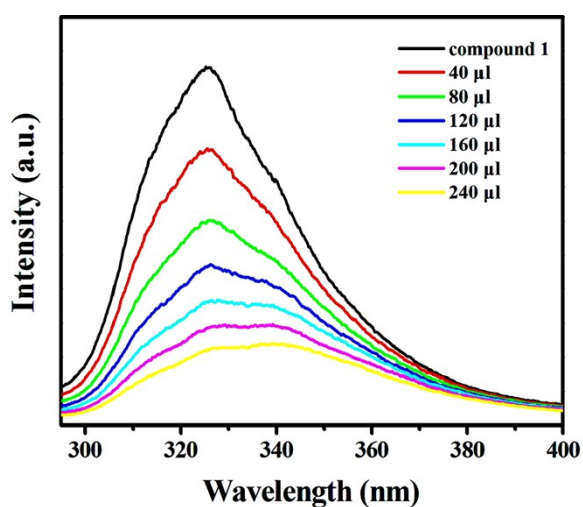


Fig. S20 The fluorescence properties of compound 1 suspension in the presence of various contents of p-nitrophenol.

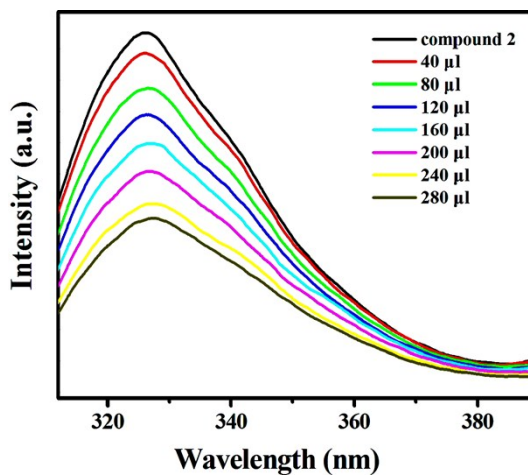


Fig. S21 The fluorescence properties of compound **2** suspension in the presence of various contents of 4-nitrotoluene.

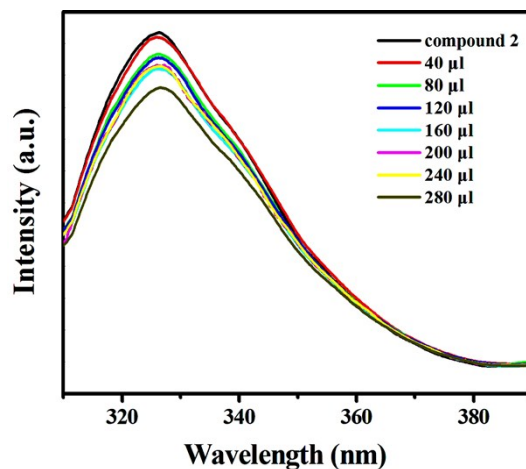


Fig. S22 The fluorescence properties of compound **2** suspension in the presence of various contents of 2,6-dinitrotoluene.

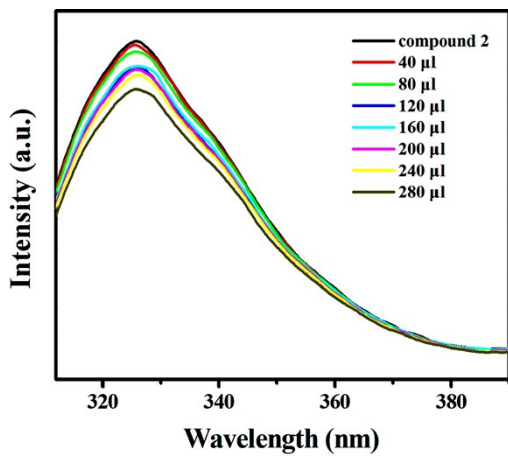


Fig. S23 The fluorescence properties of compound 2 suspension in the presence of various contents of m-dinitrobenzen.

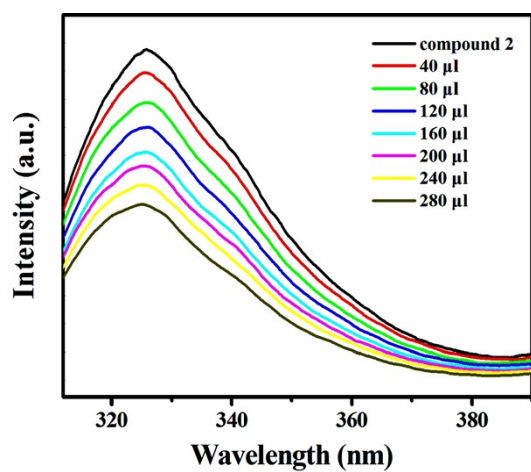


Fig. S24 The fluorescence properties of compound 2 suspension in the presence of various contents of o-nitrophenol.

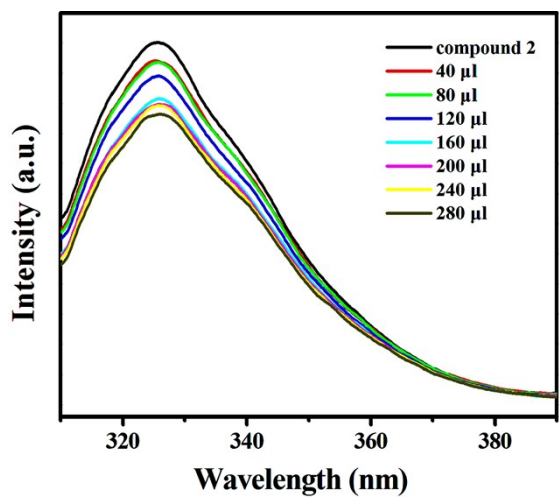


Fig. S25 The fluorescence properties of compound **2** suspension in the presence of various contents of nitromethane.

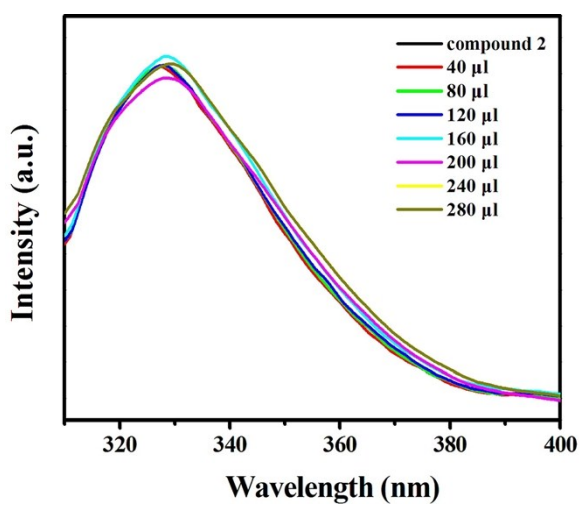


Fig. S26 The fluorescence properties of compound **2** suspension in the presence of various contents of nitrobenzene.

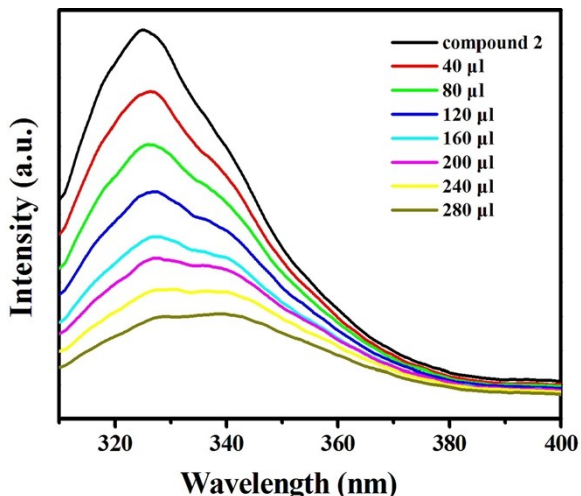


Fig. S27 The fluorescence properties of compound 2 suspension in the presence of various contents of p-nitrophenol.

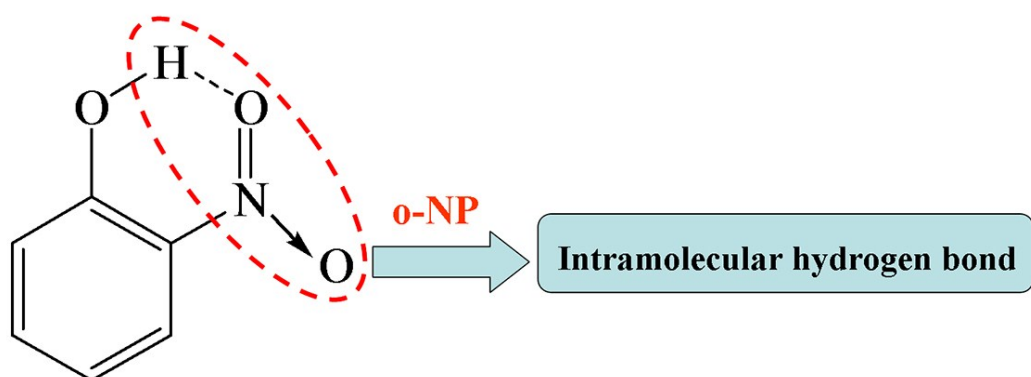


Fig. S28 The possible weak interaction mechanisms of o-nitrophenol.

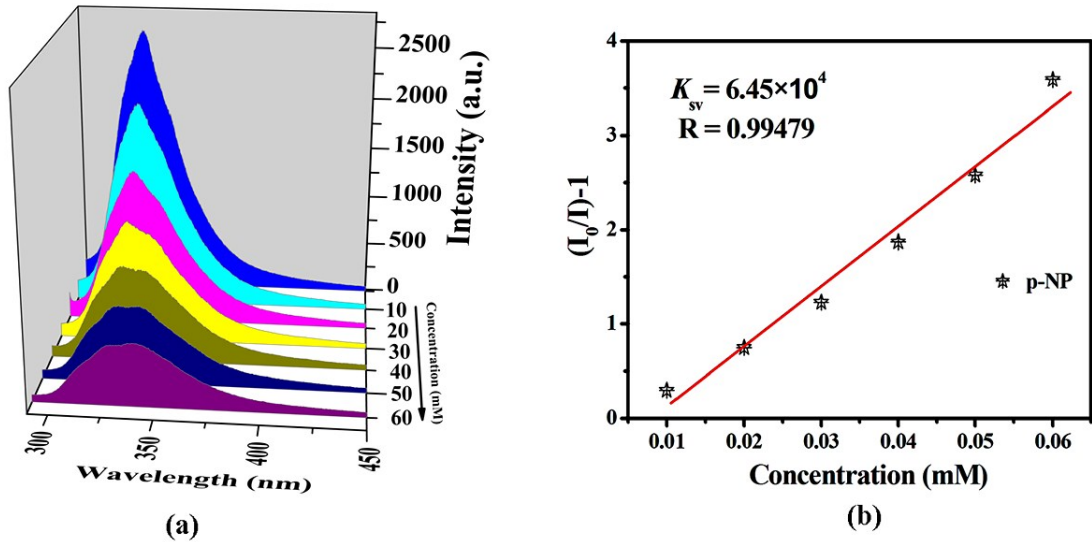


Fig. S29 (a) The luminescence spectra of compound **1** in ethanol with different concentration of p-NP; (b) The linear correlation for the plot of $(I_0/I) - 1$ vs concentration of p-NP.

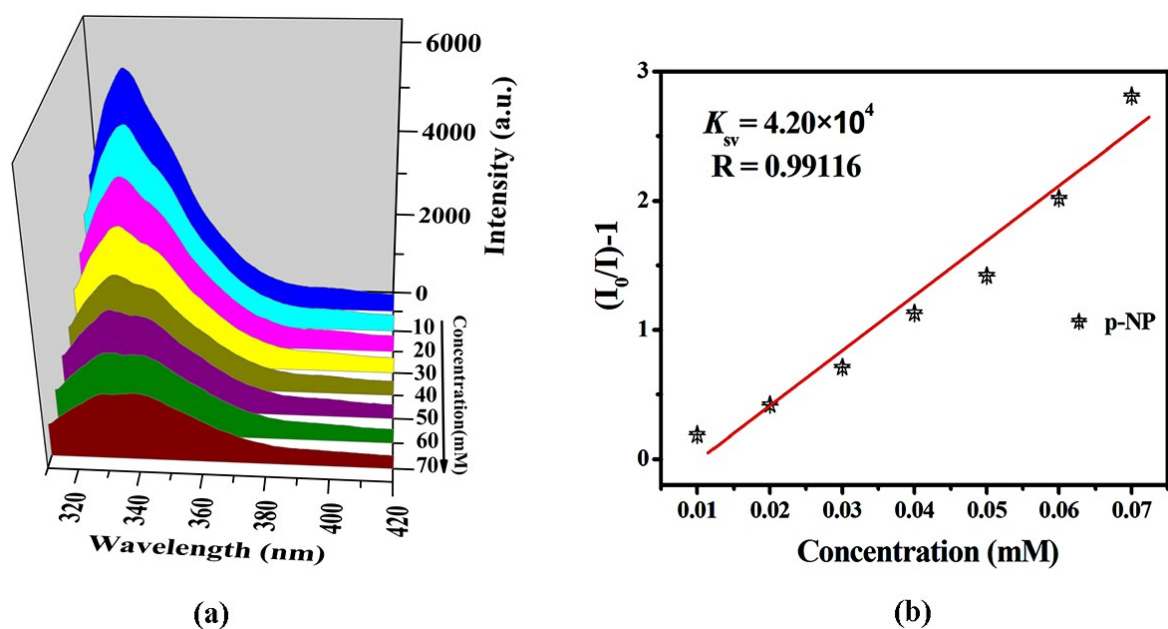


Fig. S30 (a) The luminescence spectra of compound **2** in ethanol with different concentration of p-NP; (b) The

linear correlation for the plot of $(I_0/I) - 1$ vs concentration of p-NP.

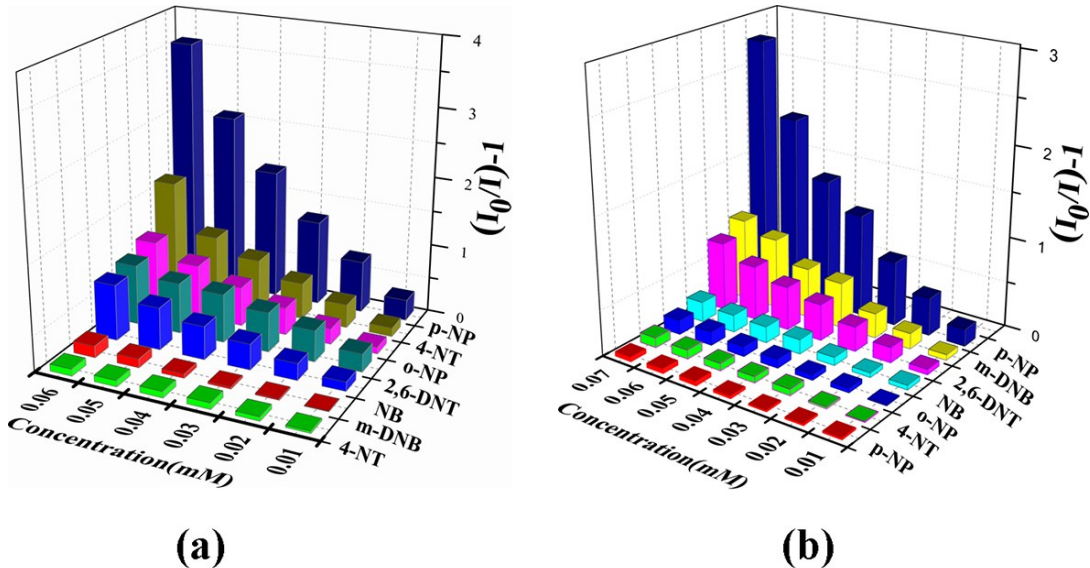


Fig. S31 Stern–Volmer plots for the fluorescence quenching of compound **1** (a) and **2** (b) (as a stable suspension in ethanol) upon gradual addition of various NACs.

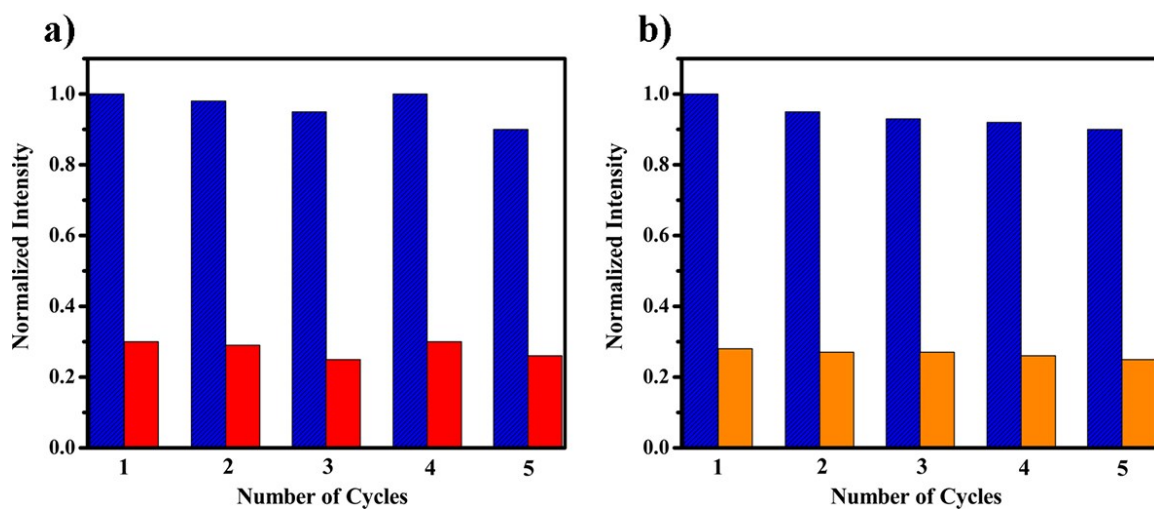


Fig. S32 The reproducibility of the quenching efficiency of the ethanol suspension of compounds **1** (a) and **2** (b) towards 4 mM p-NP solution.

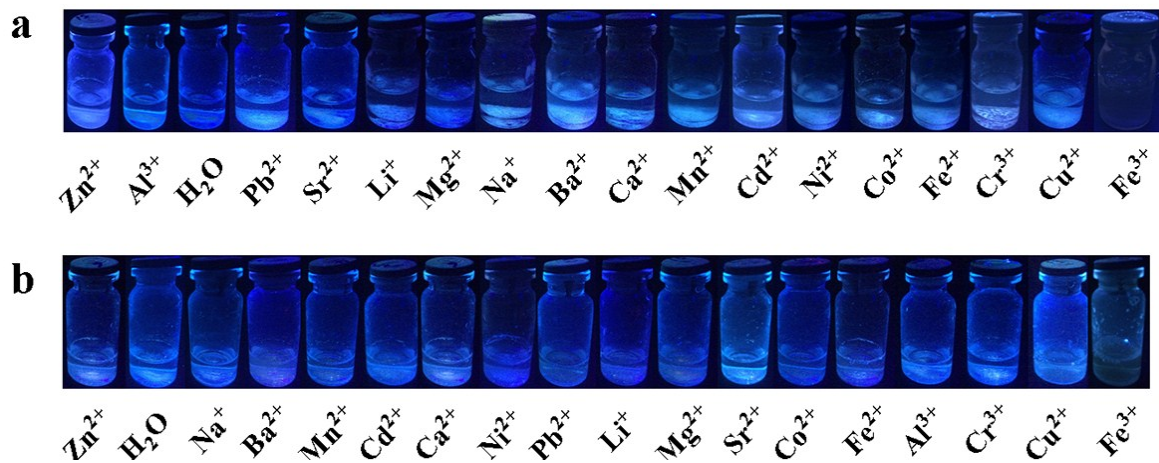


Fig. S33 The color change of the luminescent responses for sensing the different metal ions ($M = \text{Zn}^{2+}, \text{Al}^{3+}, \text{Pb}^{2+}, \text{Sr}^{2+}, \text{Li}^{+}, \text{Mg}^{2+}, \text{Na}^{+}, \text{Ba}^{2+}, \text{Ca}^{2+}, \text{Mn}^{2+}, \text{Cd}^{2+}, \text{Ni}^{2+}, \text{Co}^{2+}, \text{Fe}^{2+}, \text{Cr}^{3+}, \text{Cu}^{2+}$ and Fe^{3+}) in aqueous solution for (a) **1**, (b) **2** by the ultraviolet light.

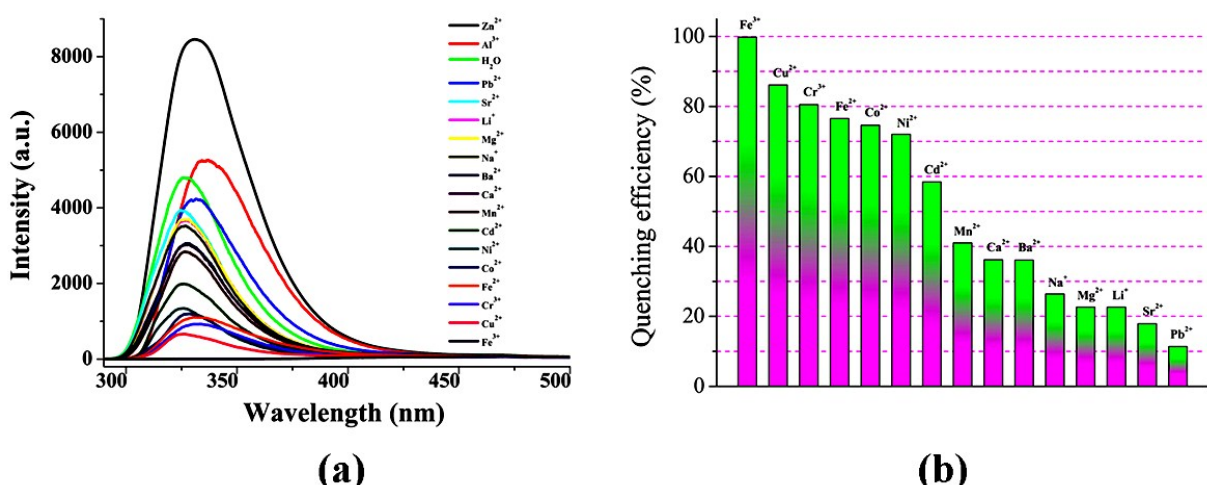


Fig. S34 (a) The luminescent intensity compound **1** treated with 1.0×10^{-3} M various cations for 12 h; (b) Percentage of fluorescence quenching by introducing different metal cations aqueous solution.

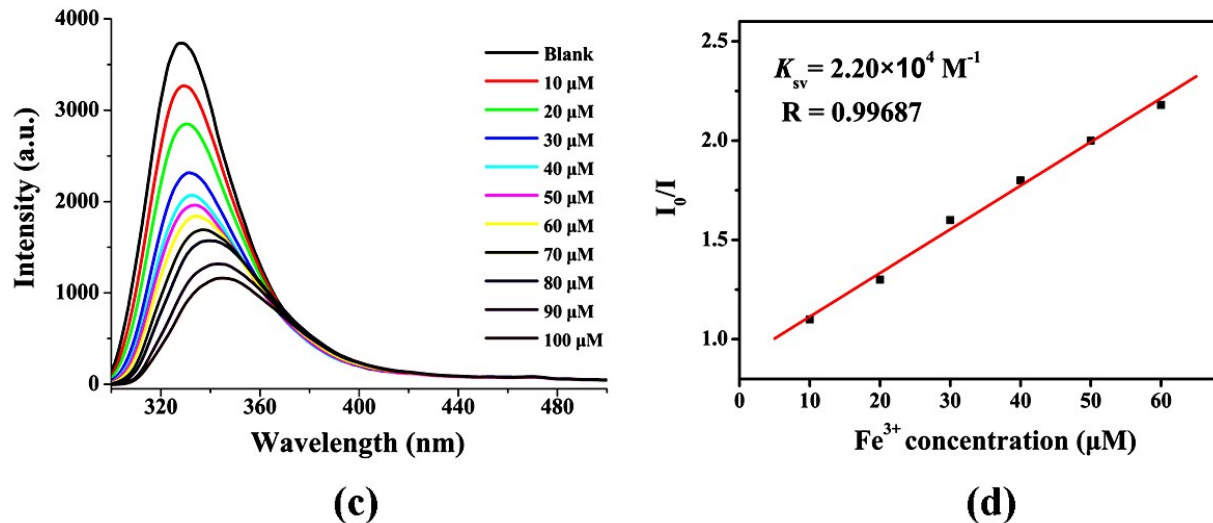


Fig. S35 (c) The luminescent spectra of compound **1** in the presence of Fe^{3+} ion with different concentrations (10–100 μM); (d) Stern–Volmer plot of I_0/I versus the Fe^{3+} concentration.

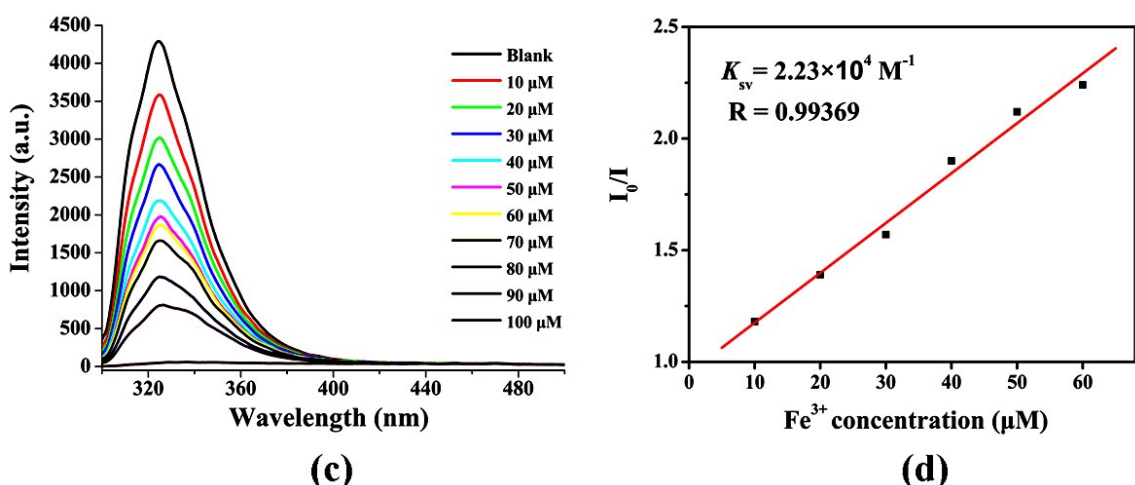


Fig. S36 (c) The luminescent spectra of compound **2** in the presence of Fe^{3+} ion with different concentrations (10–100 μM); (d) Stern–Volmer plot of I_0/I versus the Fe^{3+} concentration.

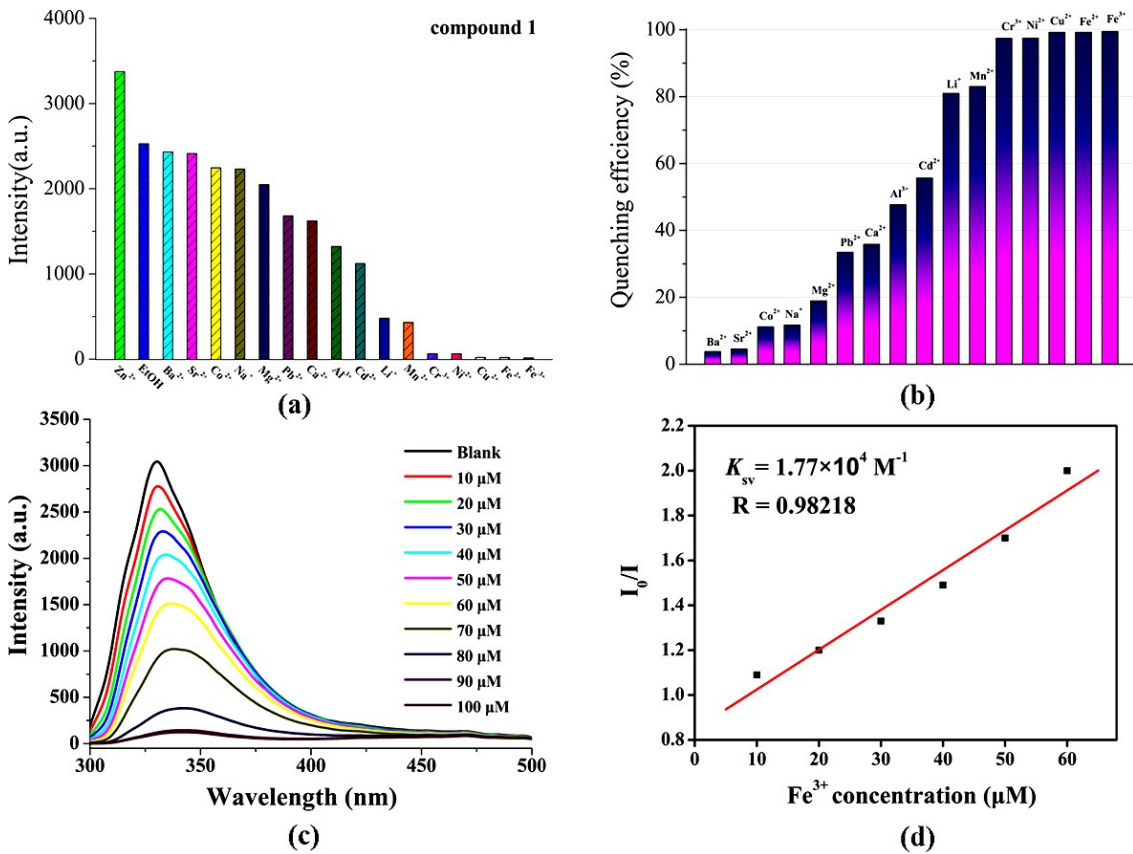


Fig. S37 (a) The luminescent intensity compound **1** treated with 1.0×10^{-3} M various cations for 12 h; (b) Percentage of fluorescence quenching by introducing different metal cations ethanol solution; (c) The luminescent spectra of compound **1** in the presence of Fe^{3+} ion with different concentrations (10–100 μM). (d) Stern–Volmer plot of I_0/I versus the Fe^{3+} concentration.

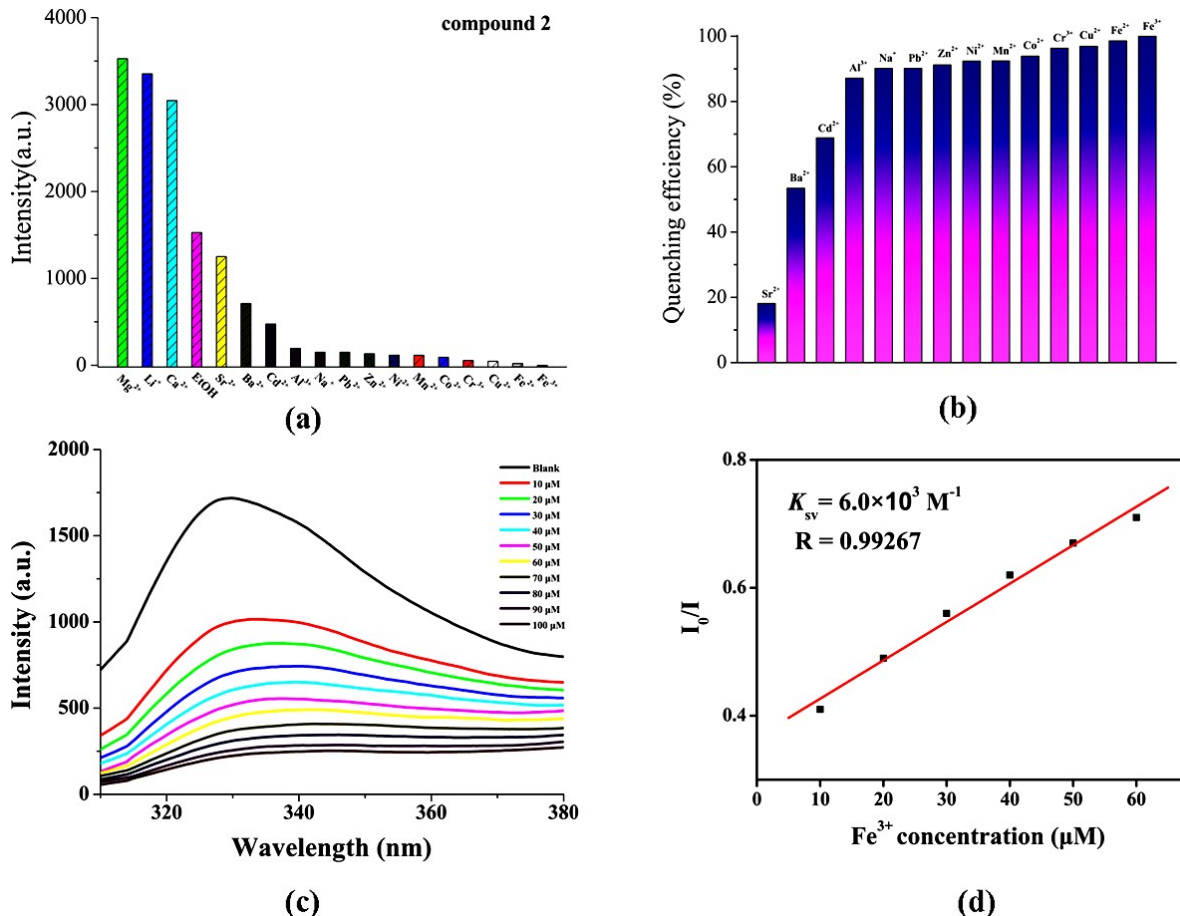


Fig. S38 (a) The luminescent intensity compound **2** treated with 1.0×10^{-3} M various cations for 12 h; (b) Percentage of fluorescence quenching by introducing different metal cations ethanol solution; (c) The luminescent spectra of compound **2** in the presence of Fe^{3+} ion with different concentrations (10–100 μM). (d) Stern–Volmer plot of I_0/I versus the Fe^{3+} concentration.

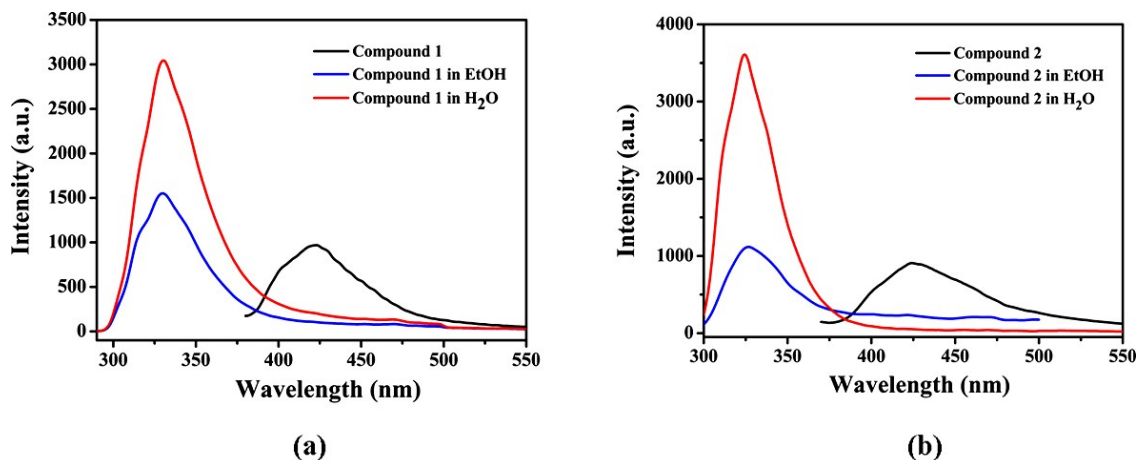


Fig. S39 The room temperature emission spectra of compounds **1** (a) and **2** (b) in ethanol and aqueous solution.

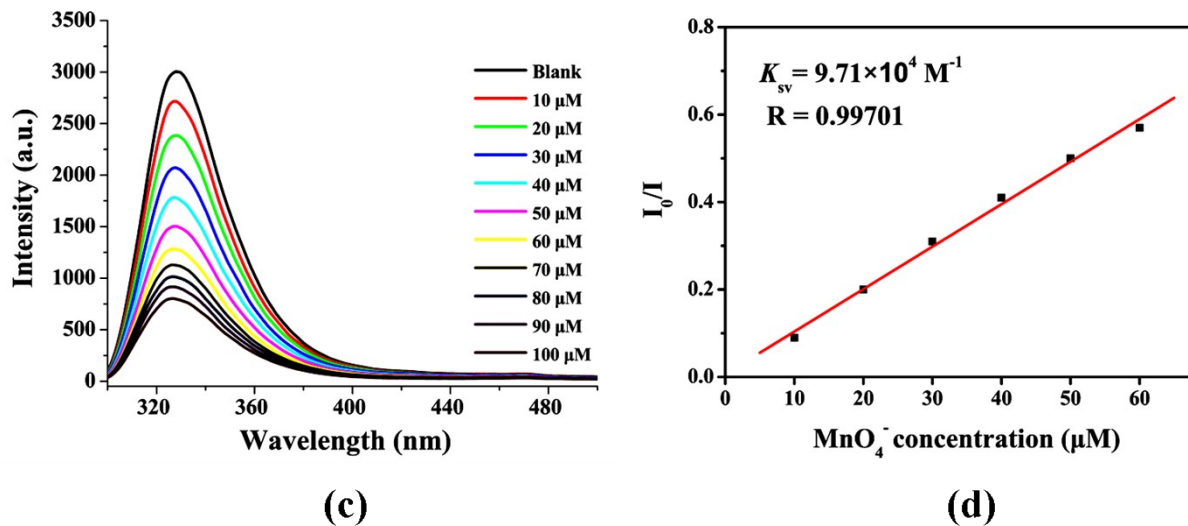


Fig. S40 (c) The luminescent spectra of compound **1** in the presence of MnO₄⁻ ion with different concentrations (10–100 μM); (d) Stern–Volmer plot of I₀/I versus the MnO₄⁻ concentration.

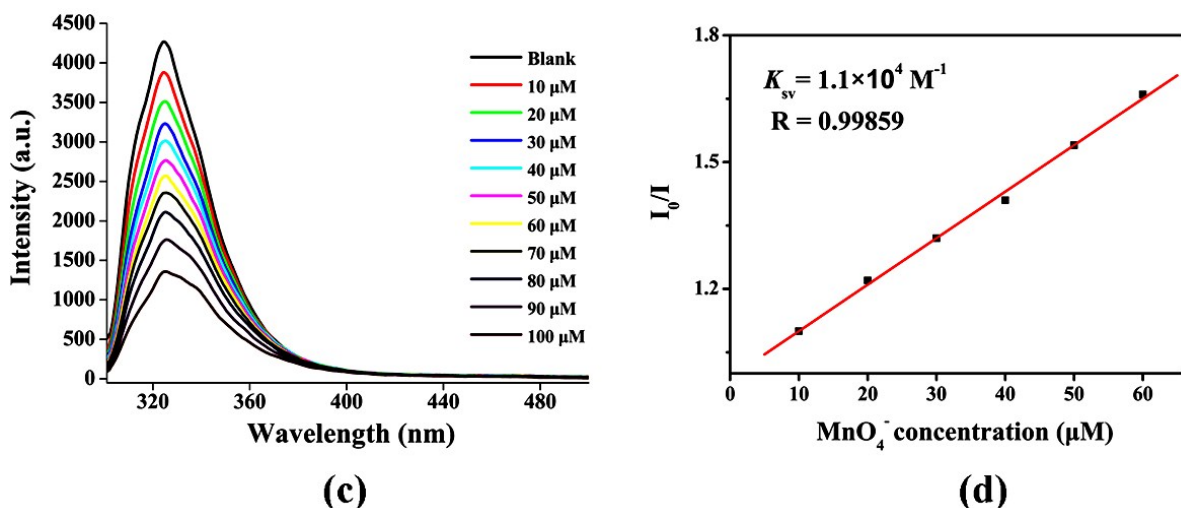


Fig. S41 (c) The luminescent spectra of compound **2** in the presence of MnO₄⁻ ion with different concentrations (10–100 μM); (d) Stern–Volmer plot of I₀/I versus the MnO₄⁻ concentration.

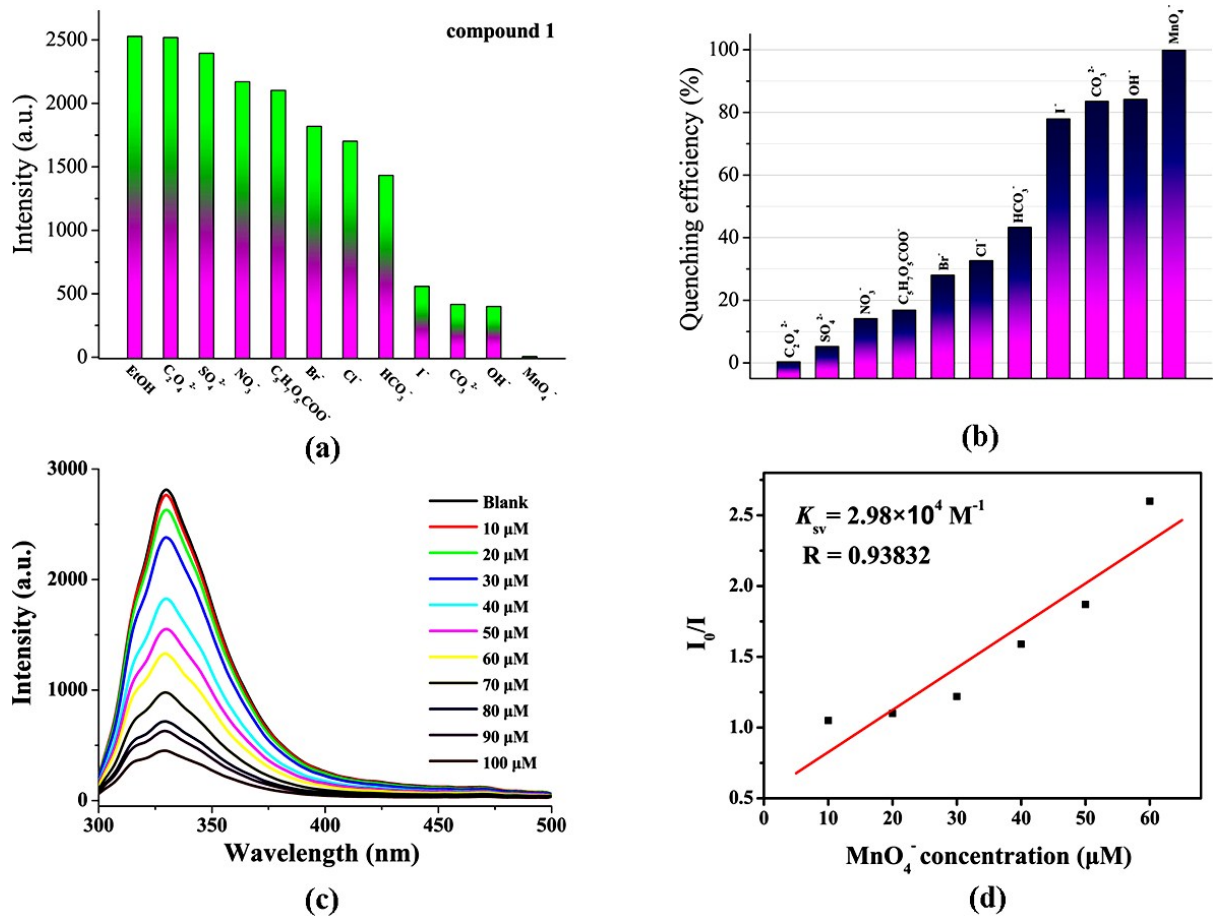


Fig. S42 (a) The luminescent intensity compound **1** treated with 1.0×10^{-3} M various anions for 12 h; (b) Percentage of fluorescence quenching by introducing different anions ethanol solution; (c) The luminescent spectra of compound **1** in the presence of MnO4^- ion with different concentrations (10–100 μ M); (d) Stern–Volmer plot of I_0/I versus the MnO4^- concentration.

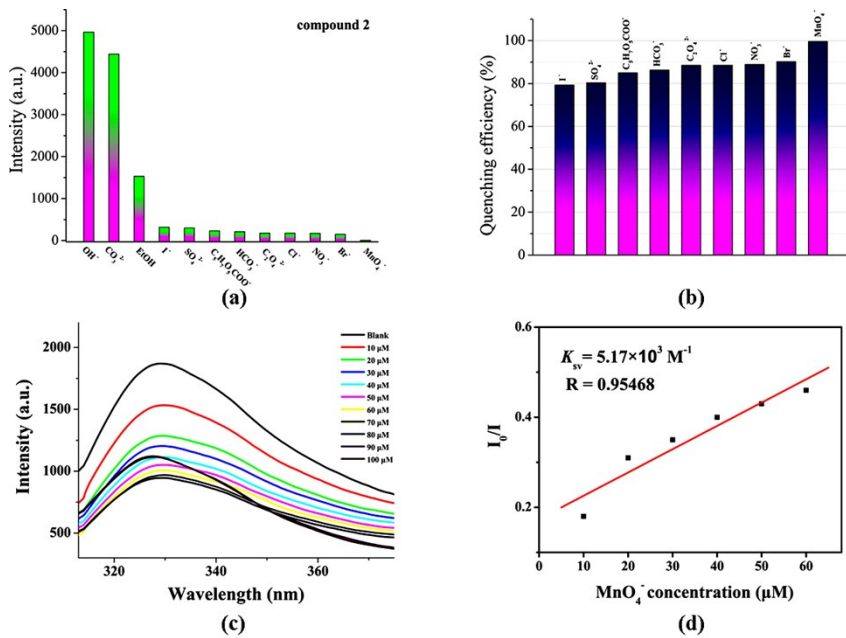


Fig. S43 (a) The luminescent intensity compound **2** treated with 1.0×10^{-3} M various anions for 12 h; (b) Percentage of fluorescence quenching by introducing different anions ethanol solution; (c) The luminescent spectra of compound **2** in the presence of MnO₄⁻ ion with different concentrations (10–100 μ M); (d) Stern–Volmer plot of I₀/I versus the MnO₄⁻ concentration.

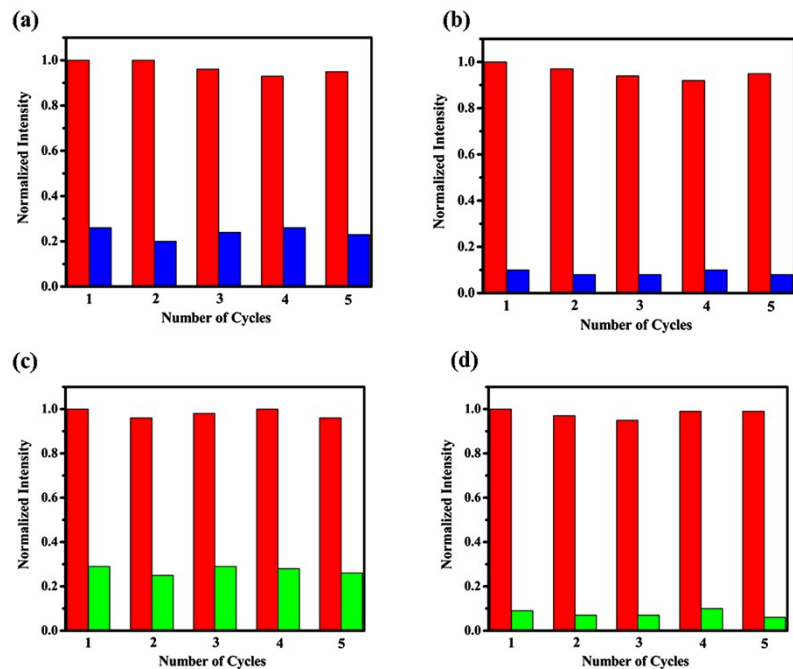


Fig. S44 (a), (c) The quenching and recovery test of compound **1** dispersed in aqueous solution in the presence of Fe^{3+} and MnO_4^- solution; (b) (d) the quenching and recovery test of compound **2** dispersed in aqueous solution in the Fe^{3+} and MnO_4^- solution. Red bar: emission of sample before sensing of Fe^{3+} and MnO_4^- ; Blue and green bars: emission of sample after sensing of Fe^{3+} and MnO_4^- respectively.

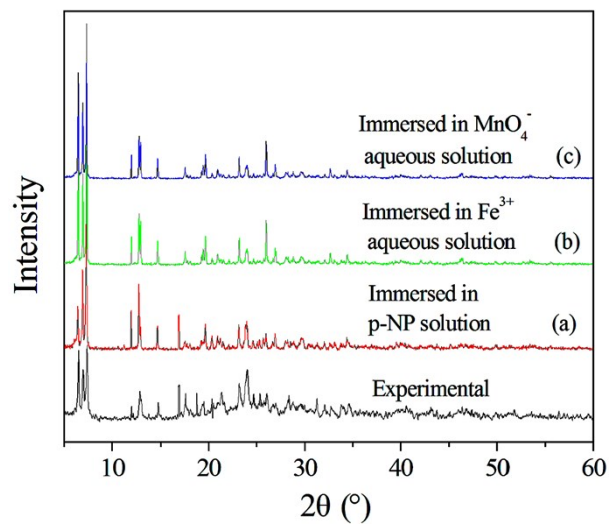


Fig. S45 The XRD patterns of compound **1** before and after treatment with p-NP (a), Fe^{3+} (b) and MnO_4^- (c) solutions.

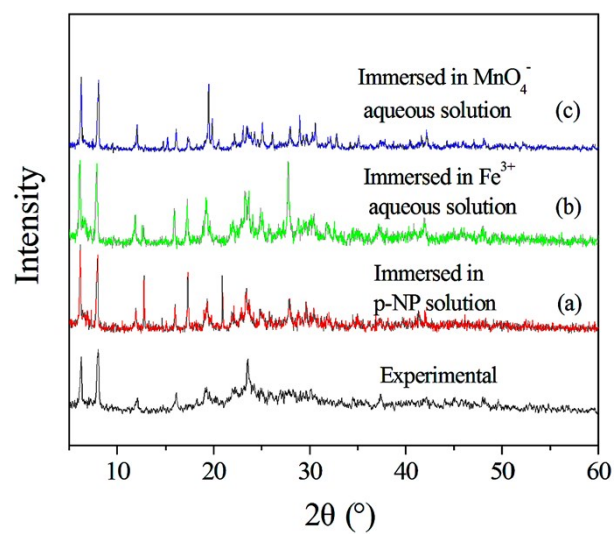


Fig. S46 The XRD patterns of compound **2** before and after treatment with p-NP (a), Fe^{3+} (b) and MnO_4^- (c) solutions.

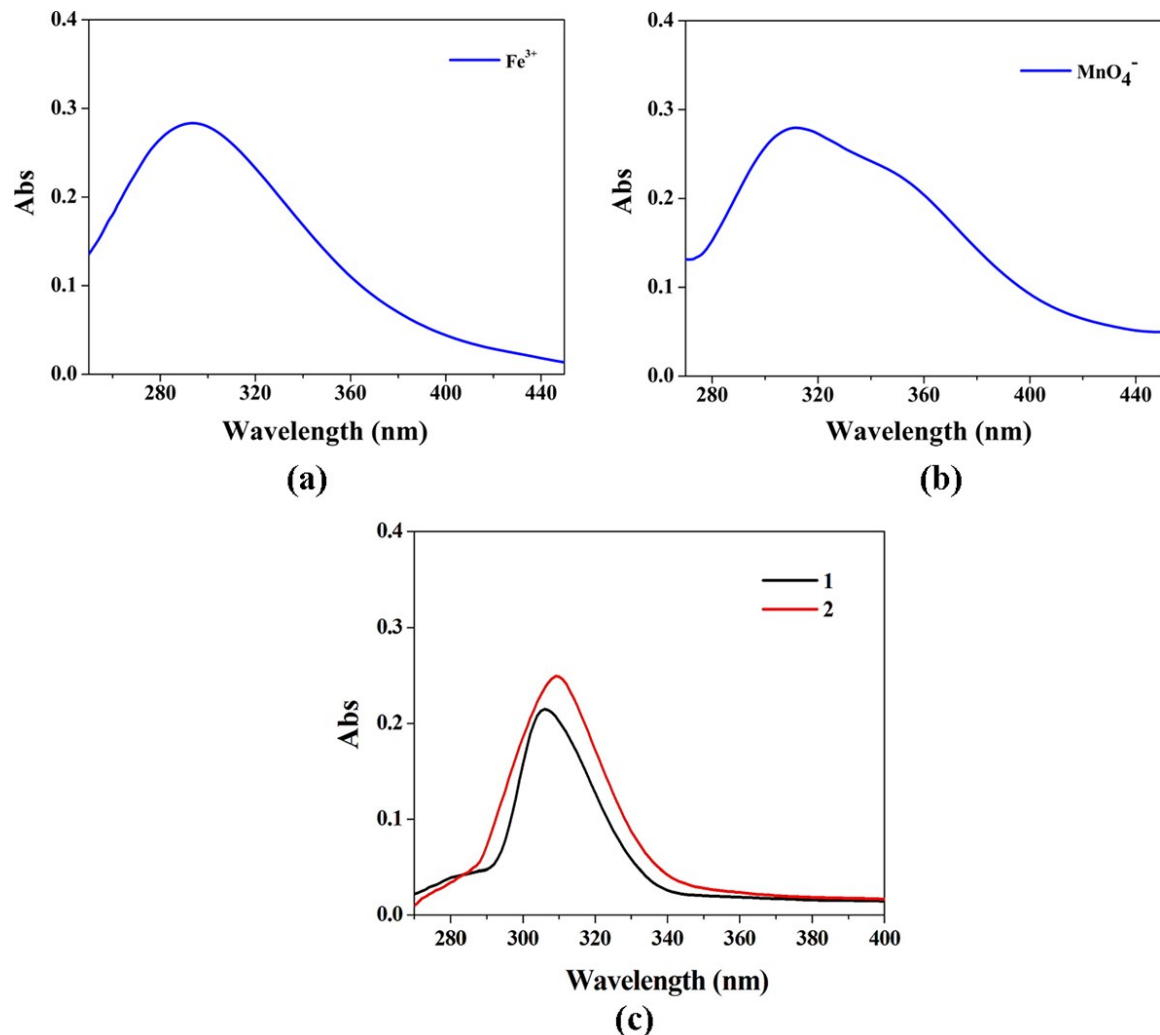
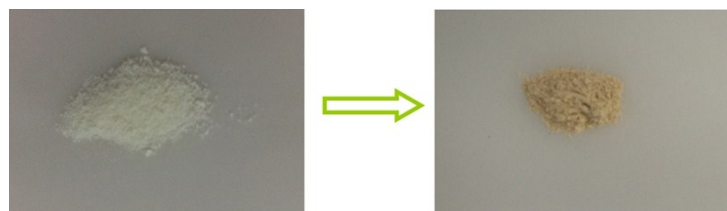
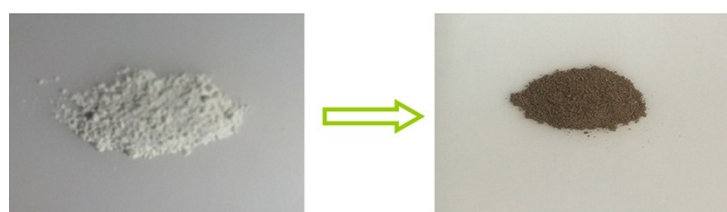


Fig. S47 UV-Vis absorption spectra of the Fe^{3+} (a), MnO_4^- (b) in aqueous solutions and compounds **1** and **2** (c).

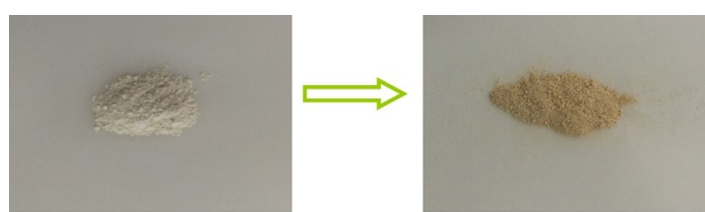


(a)

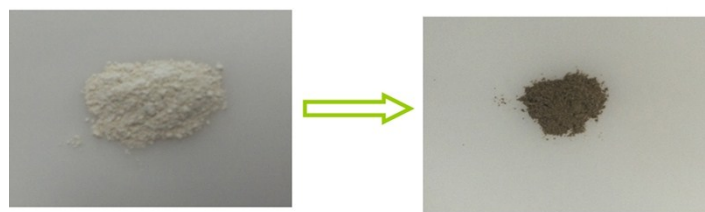


(b)

Fig. S48 The solid sample color change of compound **1** immersed into the Fe^{3+} (a) and MnO_4^- (b) aqueous solutions.



(a)



(b)

Fig. S49 The solid sample color change of compound **2** soaked in the Fe^{3+} (a) and MnO_4^- (b) aqueous solutions.

